第 26 卷第 8 期 无 机 化 学 学 报 Vol.26 No.8
2010 年 8 月 CHINESE JOURNAL OF INORGANIC CHEMISTRY 1375-1381

微波固相剥离法制备功能化石墨烯及其电化学电容性能研究

薛露平[1] 郑明波[2] 沈辰飞[1] 吕洪岭[1] 李念武[1] 潘力佳[2] 曹洁明*,[1]
([1]南京航空航天大学材料科学与技术学院纳米材料研究所,南京 210016)
([2]南京大学微结构国家实验室电子科学与工程学院,南京 210093)

摘要:通过微波固相剥离氧化石墨制备了功能化石墨烯材料。石墨烯的剥离,是由于微波加热过程中氧化石墨烯片上的官能团分解为 CO_2 和 H_2O,产生的压力超过了片层间的范德华力。形貌表征显示了石墨烯的有效剥离和纳米孔结构的形成。红外光谱分析结果表明微波剥离的功能化石墨烯仍然有少量的官能团残留。N_2 等温吸附-脱附测试结果表明样品具有高比表面积(412.9 $m^2\cdot g^{-1}$)和大孔容(1.91 $cm^3\cdot g^{-1}$)。电化学测试结果表明功能化石墨烯具有良好的电化学电容行为和 207.5 $F\cdot g^{-1}$ 的比电容。

关键词:功能化石墨烯;微波辐射;超级电容器;电化学测试
中图分类号:O613.71 **文献标识码**:A **文章编号**:1001-4861(2010)08-1375-07

Preparation of Functionalized Graphene Sheets via Microwave-Assisted Solid-State Process and Their Electrochemical Capacitive Behaviors

XUE Lu-Ping[1] ZHENG Ming-Bo[2] SHEN Chen-Fei[1] LÜ Hong-Ling[1] LI Nian-Wu[1]
PAN Li-Jia[2] CAO Jie-Ming*,[1]
([1]*Nanomaterials Research Institute, College of Materials Science and Technology, Nanjing University of Aeronautics and Astronautics, Nanjing* 210016)
([2]*National Laboratory of Microstructures, School of Electronic Science and Engineering, Nanjing University, Nanjing* 210093)

Abstract: Functionalized graphene sheets were produced by microwave-induced exfoliation of graphene oxide. Exfoliation happens when the oxygen-containing groups decomposed into CO_2 and H_2O by microwave-heat, thus yielding pressures that exceed the Van der Waals attraction between the layers. X-ray diffraction, FTIR, SEM, TEM and nitrogen adsorption-desorption were used to characterize the samples. Scanning electron microscopy images show that the sample possesses nanoporous structures. Fourier-transform infrared spectroscopy characterization proves the existence of a few functional groups on the surface of graphene sheets. The results of nitrogen adsorption-desorption analysis indicate that the sample has high BET surface area (412.9 $m^2\cdot g^{-1}$) and large pore volume (1.91 $cm^3\cdot g^{-1}$). The electrochemical tests show that the sample has good electrochemical capacitive behavior and high specific capacitance values about 207.5 $F\cdot g^{-1}$ in aqueous KOH.

Key words: functionalized graphene sheets; microwave irradiation; supercapacitor; electrochemical measurements

Graphene, an entirely new class of carbon with two dimensional (2D) structure, was first reported by Andre Geim and Kostya Novoselov in 2004[1]. Graphene has attracted great interest because of the unique physical, chemical, and mechanical properties arising from its 2D form[2-4]. Its special nanostructure holds great promise

收稿日期:2010-04-19。收修改稿日期:2010-05-22。
国家自然科学基金(No.6076019),江苏省自然科学基金(No.BK2006195),NCET 资助项目。
*通讯联系人。E-mail:jmcao@nuaa.edu.cn
第一作者:薛露平,男,25 岁,硕士研究生;研究方向:纳米材料。

for potential applications, such as energy-storage materials [5-7], composite materials [8-11], mechanical resonators [12-13], and transistors [13-17]. However, it is a challenge to produce graphene on large scale. Micromechanical cleavage of graphite to obtain graphene sheets was first reported in 2004 [1], but this method is not amenable to large-scale production of graphene. Recently, several promising methods for mass production of graphene sheets have been reported [17-26]. Chemically converted graphene sheets were prepared by the chemical reduction of exfoliated graphene oxide (GO) with reducing agents [17-20]. Stoller et al. prepared graphene sheets by means of suspending GO in water and chemical reducing with hydrazine [20]. This kind of graphene has some great performances, such as good conductivity and good supercapacitive properties (the specific capacitance of the sample was about 135 $F \cdot g^{-1}$ at a discharge current of 10 mA in 5.5 $mol \cdot L^{-1}$ KOH aqueous solution). Functionalized graphene sheets (FGS) were reported to be prepared via high temperature expansion of GO or a low-temperature reduction under high vacuum [18-21]. Malesevic et al. produced few-layer graphene via microwave plasma-enhanced chemical vapor deposition (MW-PECVD) [25]. However, high temperature or long reduction time is required for most of the methods listed above. For instance, the chemical reduction to exfoliated GO with reducing agents provides a meaningful approach to produce large-scale graphene sheets [17-20], but in most chemical reduction methods heating to nearly 100 ℃ for several hours is necessary. As for the MW-PECVD method, heating substrates to 700 ℃ is required [22]. Furthermore, the thermal exfoliation of GO usually requires high temperature (above 1 000 ℃)[21-22] or extreme exfoliation condition (vacuum) [24]. Therefore, rapid exfoliation of GO under a mild condition is needed for the preparation of FGS in large quantity. Cote et al. produced graphene sheets by flash irradiation using GO as precursor [23]. Thermal exfoliation of graphite intercalation compounds was reported by Falcao et al. using microwaves as a heat source[27]. Microwave irradiation has also been used for the synthesis of graphene sheets in solvents [28-29]. Hassan et al. produced graphene sheets supporting metal nanocrystals in aqueous and organic media by microwave irradiation [28]. The main advantage of microwave irradiation is heating the samples uniformly and rapidly compared with other conventional heating methods. Here, the thermal reduction of GO is studied using microwave irradiation as heat source.

More recently, many studies on the supercapactive behavior of graphene materials have been reported [7,20,24,30]. Vivekchand et al. prepared the graphene by three different methods [7]. The highest specific capacitance value of the sample was about 117 $F \cdot g^{-1}$ in 1 $mol \cdot L^{-1}$ H_2SO_4 aqueous electrolyte. A low-temperature exfoliation approach to produce graphenes under high vacuum was reported by Lü et al[24]. The specific capacitance value of the obtained graphene materials was up to 264 $F \cdot g^{-1}$ in 5.5 $mol \cdot L^{-1}$ KOH aqueous solution without any post-treatments without any post-treatments. Wang et al. prepared the graphene materials via a gas-solid reduction process[30]. The maximum specific capacitance value of the sample was 205 $F \cdot g^{-1}$ at energy density of 28.5 $Wh \cdot kg^{-1}$ in a 30wt% KOH aqueous solution.

In this work, we prepared FGS using GO as the precursor via an easy microwave induced solid-state process and investigated its electrochemical capacitive properties. The FGS sample possesses high BET surface area and large specific capacities in aqueous KOH (2 $mol \cdot L^{-1}$) electrolyte. The microwave-induced exfoliation approach provides a promising approach for mass production of graphenes at low cost. Moreover, the FGS products show great potential applications in electrochemical energy storage.

1 Experimental section

1.1 Preparation of FGS

GO was prepared from natural graphite powders (universal grade, 99.985%) according to hummers method [31-32]. Simply, natural graphite powders were washed by 5% HCl twice, then filtered with distilled water, and dried at 110 ℃. 10 g of washed graphite powder was added to cold (0 ℃) concentrated H_2SO_4 30 g of $KMnO_4$ was added gradually with stirring and cooling, so that the temperature of the mixture was

controlled at not higher than 20 ℃. The mixture was stirred at 35 ℃ for 30 min, then 460 mL distilled water was added slowly to the reaction vessel to cause an increase in temperature to 90 ℃ and the mixture was continued to be stirred for 15 min. Finally, 1.4 L distilled water and 100 mL 30% H_2O_2 solution were added. After the reaction, the solution was held at room temperature for 24 h. The solid product was separated by vacuum filtration, washed with 5% HCl aqueous solution until sulfate could not be detected with $BaCl_2$, then the reaction product was dried under vacuum at 50 ℃ for 48 h. Small amounts of the dried GO were added into a porcelain dish, then, the porcelain dish was placed inside a household microwave oven (G8023CSK-K3 2450 MHz, 800 W) and irradiated at full power for different time in range of 30~240 s. The obtained samples were denoted as FGS1 (30 s), FGS2 (1 min), FGS3 (2 min), and FGS4 (4 min).

1.2 Characterization

X-ray diffraction patterns were performed by a Bruker D8-advance diffractometer equipped with graphite monochromatized Cu $K\alpha$, radiation(λ=0.154 05 nm). The morphology of FGS was observed by transmission electron microscopy (TEM) (JEOL JEM-2100) and scanning electron microscopy (SEM) (Gemini, LEO 1530). Nitrogen adsorption-desorption was measured with a Micromeritics ASAP2010 instrument. Fourier transform infrared (FTIR) spectroscopy was performed with a Nicolet-670 FTIR spectrometer using the KBr pellet method.

1.3 Electrochemical tests

The electrochemical performance of FGS was evaluated by cyclic voltammetry (CV), galvanostatic charge-discharge (GC), and electrochemical impedance spectroscopy (EIS), which were done in a three-electrode experimental setup using 2 mol·L^{-1} KOH aqueous solution as the electrolyte. The prepared electrode was used as the working electrode. A platinum sheet and a saturated calomel electrode were used as counter and reference electrode, respectively. The working electrode was prepared as follows: 80wt% FGS, 15wt% acetylene black, and 5wt% polytetrufluoroethylene were well mixed and pressed onto a nickel grid (1 cm^2), and flaked under 10 MPa after being dried at 353 K for 12 h. The electrode contained about 5 mg of FGS. The CV, GC, and EIS measurements were carried out on CHI660C electrochemical workstation at room temperature. The potential rang of CV and GC was determined between -1.0 and −0.2 V (vs.SCE). The GC measurement was carried out in current density range of 1~10 A·g^{-1}. The impedance spectroscopy measurement was performed with a frequency range of 100 kHz~0.01 Hz(amplitude of 5 mV at open circuit potential).

2 Results and discussion

2.1 Characterization of FGS

Since GO is the oxidation production of pristine graphite, there are many functional groups on the surface of its carbon sheets, such as hydroxyl, carboxyl, and epoxyl groups. Fig.1 shows XRD patterns of the parent graphite, GO, FGS1, and FGS3. Compared with the pristine graphite, the native graphite peak disappears, and the feature diffraction peak of GO appears at 10.4°, corresponding to an interlayer spacing (*d*-spacing) of 0.85 nm, which indicates the complete oxidation of the starting graphite and most oxygen is bonded to the planar surface of graphite after the oxidization [33]. After the microwave-heating treatment, the sharp peak around 10° at the XRD patterns disappears, indicating that oxygen intercalated into the interlayer spacing of graphite is largely removed by microwave irradiation. In Fig.1, FGS samples display amorphous structure patterns.

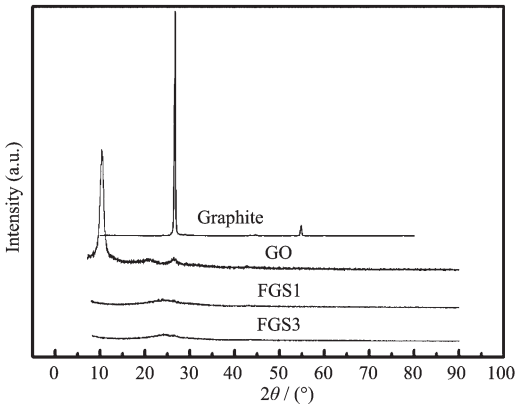

Fig.1　XRD patterns of graphite, pristine GO, FGS1 and FGS3

Fig.2 shows the FTIR spectra of GO, FGS1, and FGS3. In addition to a broad band (3 427 cm^{-1}) due to -OH groups[34], the characteristic peaks appear at 1 734, 1 624, 1 400, 1 228, and 1 050 cm^{-1} can be assigned to the C=O, aromatic C=C, carboxy C-O, epoxy C-O, and C-O groups on the surface of the GO layers. Compared with the pristine GO, the intensity of the peaks at 1 734 and 1 624 cm^{-1} for FGS samples decrease, and the peaks at 1 400 and 1 050 cm^{-1} disappear, which indicates that microwave irradiation removes most of the functional groups on the surface of the GO layers and still leaves a few residual functional groups on the surface of graphene sheets.

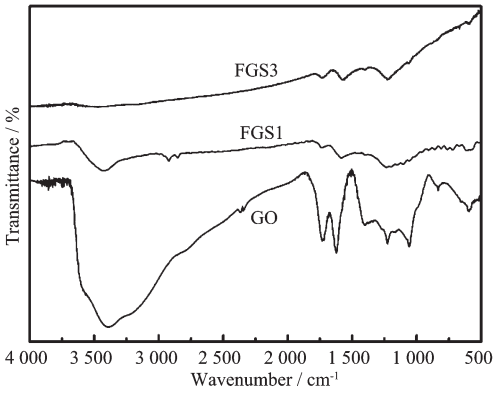

Fig.2 FTIR spectra of GO, FGS1, and FGS3

Low-magnification scanning electron microscopy (SEM) image (Fig.3(a)) of FGS3 shows that the sample has many nanopores between the sheets, which results from the thermal exfoliation of GO. The nanoporous structure formed after the pressure generated by the decomposition of oxygen-containing groups via microwave-heat was enough to overcome the Van der Waals forces binding the GO sheets together. The high magnification SEM and transmission electron microscopy (TEM) images (Fig.3 (b) and Fig.3 (c)) of FGS3 show a wrinkled paper-like structure of the ultrathin graphene sheets and stacking of sheets. In Fig.3 (d), the selected area electron diffraction shows only weak and diffuse rings, which indicates that the graphene sheets lose the long range ordering.

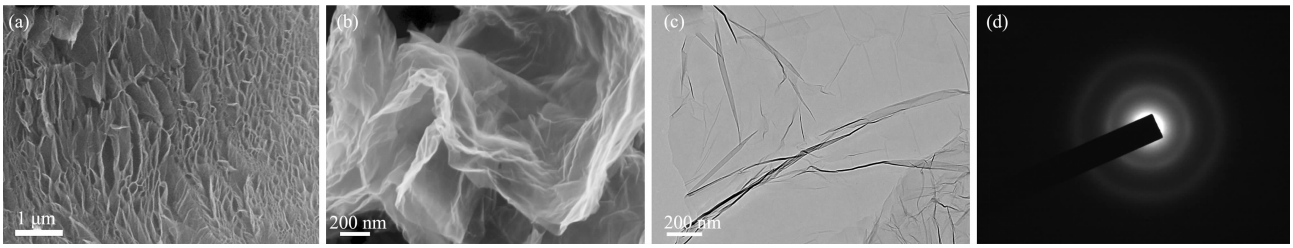

Fig.3 SEM images of FGS3 (a, b), TEM and selected area electron diffraction pattern (SAED) of FGS3 (c, d)

The results of nitrogen adsorption-desorption analysis (Fig.4(a)) also prove that the FGS samples have nanoporous structure. Fig.4 (b) indicates that these samples have a broad pore size distribution from 2 to 200 nm. The BET surface areas, pore volumes, and average pore sizes of the samples are shown in Table 1. It can be found that, compared with FGS3 (2 min irradiation), the BET surface areas of FGS samples have no significant change after extending the processing time. Furthermore, the BET surface areas of FGS are

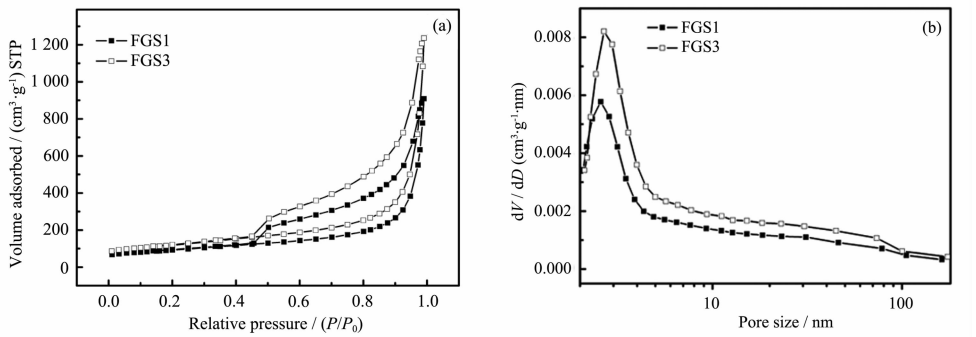

Fig.4 (a) Nitrogen adsorption-desorption isotherms of FGS1 and FGS3. (b) BJH pore size distributions from adsorption branches for FGS1 and FGS3

Table 1　BET surface areas, pore volumes, and average pore sizes of the FGS samples

Sample	BET surface area / ($m^2 \cdot g^{-1}$)	Pore volume / ($cm^3 \cdot g^{-1}$)	Average pore size / nm
FGS1	319.7	1.41	17.6
FGS2	338.2	1.53	18.1
FGS3	412.9	1.91	18.5
FGS4	408.7	1.67	16.3

lower than the theoretical limit (2 630 $m^2 \cdot g^{-1}$) of graphene[23]. It indicates that the FGS products contain extensive domains of stacked graphitic layers.

2.2　Electrochemical testing

The supercapacitive behavior of FGS3 is analyzed using cyclic voltammetry (CV), galvanostatic charge-discharge (GC), and electrochemical impedance spectroscopy (EIS), which are done in a three-electrode system in aqueous KOH (2 $mol \cdot L^{-1}$) electrolyte. Fig.5(a) shows the CV curves of FGS3 with different scan rates (5~50 $mV \cdot s^{-1}$). At a relatively low scanning rate, the CV curves of FGS3 exhibit rectangular-like shape, even at a scanning rate as high as 50 $mV \cdot s^{-1}$, the CV curve still shows a rectangular shape with small distortion, indicating an excellent supercapacitive behavior.

Discharge curves of the sample are performed at a current density range of 1~10 $A \cdot g^{-1}$. As seen in Fig.5 (b). The specific capacitance is evaluated from the slope of the discharge curves, according to the equation: $C_m = I\Delta t/(m\Delta v)$[35], where I is the current of charge-discharge, Δt is the time of discharge, m is the mass of active materials in the working electrode, and ΔV is 0.8 V. The evaluated results (Table 2) indicate that FGS3 possesses higher capacitance retention (72.3%) at a current density of 10 $A \cdot g^{-1}$. Specific capacitance per surface unit C_{SA} ($\mu F \cdot cm^{-2}$) is calculated using equation: $C_{SA} = C_m/SA$[36], where SA is the BET surface area ($m^2 \cdot g^{-1}$). The BET surface area of mesoporous carbon CMK-

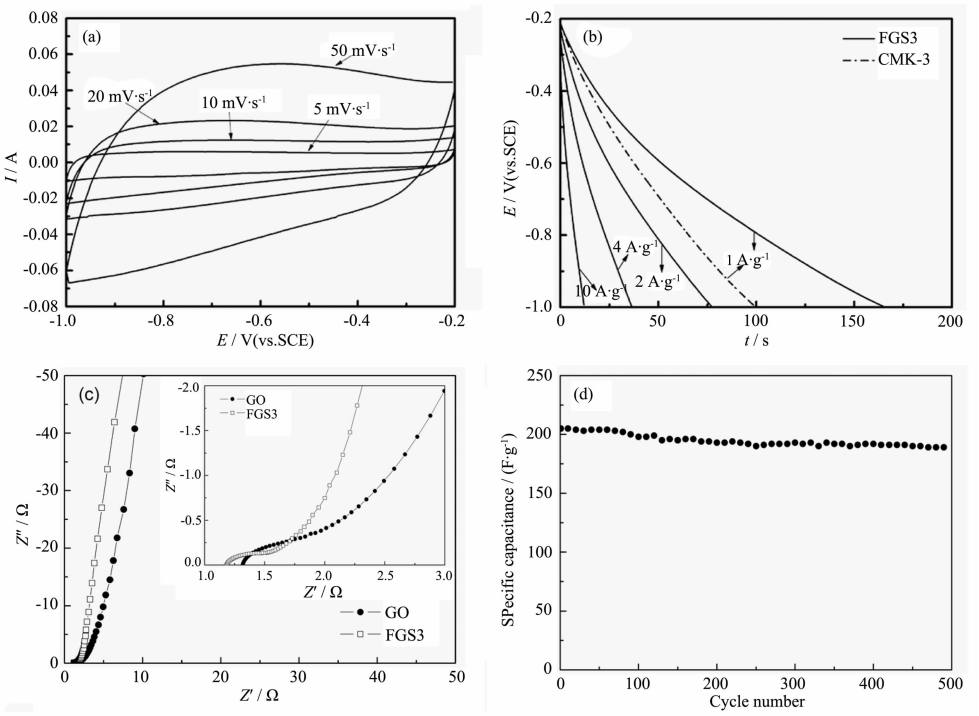

Fig.5　(a) Cyclic voltammograms of the FGS3 obtained at different scan rates. (b) Galvanostatic discharge curves of FGS3 at different current density range from 1 to 10 $A \cdot g^{-1}$ and mesoporous carbon CMK-3 at a current density of 1 $A \cdot g^{-1}$. (c) Electrochemical impedance spectra measured from 100 kHz to 0.01 Hz of the FGS3 and GO (amplitude of 5 mV at open circuit potential). Inset shows an enlarged scale. (d) Cycling performance of FGS3 (current density: 1 $A \cdot g^{-1}$).

Table 2 Specific capacitances obtained from GC methods and capacitance retention for FGS3

Sample	C_m / (F·g^{-1})				Capacitance retention / %
	1 A·g^{-1}	5 A·g^{-1}	4 A·g^{-1}	10 A·g^{-1}	
FGS3	207.5	192.5	180.1	150.0	72.3

3 is around 1 196 m^2·g^{-1} and the specific capacitance of CMK-3 at the current density of 1 A·g^{-1} is about 124.4 F·g^{-1}. The specific capacitance per surface area of FGS3 calculated is about 50.3 μF·cm^{-2} at the current density of 1 A·g^{-1}, which is much higher than 10.4 μF·cm^{-2} afforded by CMK-3.

The impedance spectra consist of a semicircle in high-frequency range and a line inclined at a constant angle to the real axis in low-frequency range. The semicircle portion observed at high frequencies corresponds to the charge transfer limiting process. As we can see from Fig.5 (c), low-down semicircles are observed at high frequency region, from the diameter of semicircle, the internal resistance of FGS3 is lower than GO. It indicates that the conductive performance of FGS3 is enhanced significantly. The inclined line in low-frequency range is attributed to Warburg impedance that is associated with electrolyte diffusion through the anode. Compared with GO, the imaginary part of the impedance spectra at low frequencies of FGS3 is much closer to a 90° line in an ideal capacitor, indicating an ideal supercapacitive behavior of FGS3. Moreover, the electrical conductivity of FGS is an effective indicator to the exfoliation extent of GO[37]. The results show the effective exfoliation of GO.

Long cycle life of supercapacitor is important for its practical applications [38-39]. Fig.4 (d) shows the variation of specic capacitance for FGS3 at a constant current density of 1 A·g^{-1}. As can be seen, the sample possesses high capacitance retention (92.2%) after 500 cycles of testing.

For the supercapacitive electrode materials, the efficient adsorption of electrolyte ions is crucial to generate high specific capacitance[40]. The morphology characterization of FGS shows that the samples have a nanoporous structure~and low degree of agglomeration. Different from conventional carbon materials used for supercapacitor, the structure of FGS allows the electrolyte ion to penetrate both the outer and inner region of the solids. Therefore, both sides of exfoliated graphene sheets could be exposed to the electrolyte and contribute to the capacitance. Furthermore, the residual functional groups on the surface of FGS may improve the hydrophilicity of electrode and afford the pseudocapacitance [41-42], thus enhancing the overall charge storage capability.

3 Conclusion

In summary, an easy, high yield, green, and fast microwave-induced solid state approach to the synthesis of FGS is reported using GO as precursor. The results of electrochemical tests indicate that the FGS sample has good supercapacitive behavior and conductivity. The present method can be used to prepare graphene sheets in large scale. The produced graphenes are expected to be used for further application in electrochemical energy storage and electrocatalysis.

References:

[1] Novoselov K S, Geim A K, Morozov S V, et al. *Science*, **2004**, **306**:666-669

[2] Dikin D A, Stankovich S, Zimney E J, et al. *Nature*, **2007**, **448**:457-460

[3] Wang G X, Yang J, Park J, et al. *J. Phys. Chem. C*, **2008**, **112**:8192-8195

[4] HUANG Gui-Rong(黄桂荣), CHEN Jian(陈 建). *Carbon Techniques*(*Tansu Jishu*), **2009**,**1**(28):35-39

[5] Novoselov K S, Jiang D, Schedin F, et al. *Proc. Natl. Acad. Sci. U.S.A*., **2005**,**102**:10451-10453

[6] Takamura T, Endo K, Fu L, et al. *T. Eletrochim. Acta*, **2007**, **53**:1055-1061

[7] Vivekchand S R C, Rout C S, Subrahmanyam K S, et al. *J. Chem. Sci*., **2008**,**120**:9-13

[8] Stankovich S, Dikin D A, Dommett G H B, et al. *Nature*, **2006**,**442**:282-286

[9] Watcharotone S, Dikin D A, Stankovich S, et al. *Nano Lett.*, **2007**,**7**:1888-1892

[10]ZHANG Xiao-Yan(张晓艳), LI Hao-Peng(李浩鹏), CUI Xiao-Li(崔晓莉). *Chinese J. Inorg. Chem.*(*Wuji Huaxue Xuebao*), **2009**,**25**(11):1903-1907

[11]Singh V K, Patra M K, Manoth M, et al. *New Carbon Mater.* (*Xinxing Tan Cailiao*), **2009**,**24**(2):147-152

[12]Bunch J S, Van Der Zande A M, Verbridge S S, et al. *Science*, **2007**,**315**:490-493

[13]Liang Y Y, Wu D Q, Feng X L, et al. *Adv. Mater.*, **2009**,**21**: 1679-1683

[14]Liang G, Neophytou N, Nikonov D E, et al. *IEEE Trans. Electron. Dev.*, **2007**,**54**:677-682

[15]Li X L, Wang X R, Zhang L, et al. *Science*, **2008**,**319**:1229-1232

[16]Yan Q M, Huang B, Yu J, et al. *Nano Lett.*, **2007**,**7**:1469-1473

[17]Stankovich S, Piner R D, Chen X, et al. *J. Mater. Chem.*, **2006**,**16**:155-158

[18]Gilije S, Han S, Wang M, et al. *Nano Lett.*, **2007**,**7**:3394-3398

[19]Fan B X, Peng W, Li Y, et al. *Adv. Mater.*, **2008**,**20**:1-4

[20]Stoller M D, Park S, Zhu Y W, et al. *Nano Lett.*, **2008**,**8**: 3498-3502

[21]Schniepp H C, Li J L, McAllister M J, et al. *J. Phys. Chem. B*, **2006**,**110**:8535-8539

[22]McAllister M J, Li J L, Adamson D H, et al. *Chem. Mater.*, **2007**,**19**:4396-4404

[23]Verdejo R, Barroso-Bujans F, Rodriguez-Perez M A, et al. *J. Mater. Chem.*, **2008**,**18**:2221-2226

[24]Lü W, Tang D M, He Y B, et al. *ACS Nano*, **2009**,**3**:3730-3736

[25]Malesevic A, Vitchev R, Schouteden K, et al. *Nanotechnology*, **2008**,**19**:305604

[26]Cote L J, Cruz-Silva R, Huang J X. *J. Am. Chem. Soc.*, **2009**, **131**:11027-11032

[27]Falcao E H L, Blair R G, Mack J J, et al. *Carbon*, **2007**,**45**: 1364-1369

[28]Hassan H M A, Abdelsayed V, Khder A S, et al. *J. Mater. Chem.*, **2009**,**19**:3832-3837

[29]Murugan A V, Muraliganth T, Manthiram A. *Chem. Mater.*, **2009**,**21**:5004-5006

[30]Wang Y, Shi Z Q, Huang Y, et al. *J. Phys. Chem. C*, **2009**, **113**:13103-13107

[31]Hummers W S, Offeman R E. *J. Am. Chem. Soc.*, **1958**,**80**: 1339-1339

[32]Liu P G, Gong K C, Xiao P, et al. *J. Mater. Chem.*, **2000**,**10**: 933-935

[33]Jeong H K, Lee Y P, Lahaye R J. et al. *J. Am. Chem. Soc.*, **2008**,**130**:1362-1366

[34]Subrahmanyam K S, Vivekchand S R C, Govindaraj A C, et al. *J. Mater. Chem.*, **2007**,**18**:1517-1523

[35]Zheng M B, Cao J, Liao S T, et al. *J. Phys. Chem. C*, **2009**, **113**:3887-3894

[36]Hulicova D, Yamashita J, Soneda Y, et al. *Chem. Mater.*, **2005**,**17**:1241-1247

[37]Guo H L, Wang X F, Qian Q Y, et al. *ACS Nano*, **2009**,**3**: 2653-2659

[38]Simon P, Gogotsi Y. *Nat. Mater.*, **2008**,**7**:845-854

[39]SUN Zhe(孙　哲), LIU Kai-Yu(刘开宇), ZHANG Hai-Feng(张海峰), et al. *Acta Phys. -Chim. Sin.* (*Wuli Huaxue Xuebao*), **2009**,**25**(10):1991-1997

[40]Futaba D N, Hata K, Yamada T, et al. *Nat. Mater.*, **2006**,**5**: 987-994

[41]WANG Xiao-Feng(王晓峰), WANG Da-Zhi(王大志), LIANG Ji(梁　吉). *Chinese J. Inorg. Chem.*(*Wuji Huaxue Xuebao*), **2003**,**19**(2):137-141

[42]Du Q L, Zheng M B, Zhang L F, et al. *Eletrochim. Acta*, **2010**,**55**:3897-3903